Nonlinear harmonic generation by internal waves in a density staircase

Scott Wunsch
Applied Physics Laboratory, Johns Hopkins University, Laurel, Maryland 20723, USA

(Received 17 May 2018; published 20 November 2018)

Recent work has explored linear internal wave transmission and reflection across a density staircase. Here, weakly nonlinear theory is used to extend previous linear internal wave solutions to include nonlinear effects at density interfaces within the staircase. Near-resonant forcing of freely propagating modes of the staircase by weakly nonlinear incident internal waves is shown to occur for some wavelength-frequency combinations. In some cases, this results in the staircase radiating double-frequency, double-wave-number harmonic waves. In others, incident waves excite one or more interfacial waves which propagate along the density interfaces within the staircase. This nonlinear effect is expected to be significant for internal waves of realistic amplitude incident on oceanic thermohaline staircases.

DOI: 10.1103/PhysRevFluids.3.114803

I. INTRODUCTION

Double-diffusive convection in the oceans can lead to the formation of a thermohaline staircase (also called double-diffusive layering) if cool fresh water lies over warmer saltier water [1–3]. The necessary conditions for staircase formation are commonly found in polar oceans [2] and observations have been reported in the Arctic [4–7] and Antarctic [8,9]. These observations indicate that the staircases typically consist of layers of well-mixed water a few meters thick but kilometers wide, separated by sharp density jumps. The layers are typically found at depths between $\sim$100 and $\sim$400 m in waters with a mean buoyancy frequency of a few cycles per hour. Staircases have also been observed in the Black Sea [10], the Mediterranean Sea [11], the tropical Atlantic Ocean [12–14], and the Red Sea [15].

In the Arctic, internal waves may play an important role in ocean dynamics [16]. Decreasing ice cover may increase internal wave activity, resulting in renewed interest in the interaction of internal waves with the thermohaline staircase. Theoretical and laboratory studies have shown that linear internal wave transmission through a staircase is strongly affected by constructive and destructive interference within the layers, resulting in transmission peaks [17,18].

In astrophysics, a similar double-diffusive layering phenomenon occurs in the interior of stars and gas giant planets, where it is known as semiconvection [19]. In this context, recent studies have explored the modes of a density staircase surrounded by convecting fluid [20] and have extended the calculation of [18] to include the full Coriolis effect on internal wave transmission through a staircase [21].

Recent work has shown that internal waves passing through a sharp density jump, as occurs at staircase layer boundaries, generate double-frequency and double-wave-number harmonics. This effect has been demonstrated in both the laboratory [22–24] and numerical simulations [25–27]. The harmonic was shown theoretically to arise due to self-interaction of the internal wave in regions where the density gradient is changing [27,28] and is a special case of resonant triads in nonuniform stratifications [29]. For incident internal wave frequencies exceeding half the far-field buoyancy frequency, the harmonic takes the form of an interfacial wave propagating horizontally along the density interface. Since the mixed-layer boundaries of the thermohaline staircase have sharp changes in the density gradient, nonlinear harmonic generation is expected to occur there.

In the thermohaline staircase, the possibility of energy transfer from incident internal waves to interfacial waves has been suggested as a possibility based on the dispersion relation [17]. Here, weakly nonlinear theory, analogous to that of [27,30], is used to extend the previous linear internal wave solution of [18] for a density staircase to include nonlinear harmonic generation at the density jumps. This leads to a weakly nonlinear theory for interfacial waves generated from incident waves as conjectured in [17]. It also describes radiated harmonic waves generated by incident waves with frequencies less than half the far-field buoyancy frequency.

The theoretical background for harmonic generation is presented in Sec. II, followed by the linear and weakly nonlinear solutions for the staircase density profile in Sec. III. The linear solution is a generalization of that of [18] but reduces to it in the appropriate limit. Results and implications for oceanic thermohaline staircases are presented in Secs. IV and V, respectively.

II. WEAKLY NONLINEAR THEORY

Using a standard theoretical framework for a Boussinesq fluid with buoyancy frequency $N(z)$ and rotation frequency f, the weakly nonlinear solution is constructed in terms of the stream function $\psi(x,z,t)$ ($u \equiv \partial_z\psi$ and $w \equiv -\partial_x\psi$). Fully three-dimensional effects are neglected, so there are no gradients in the y direction, but the y component of velocity v is nonzero due to rotation. Using the standard approximation for rotational effects (neglecting the horizontal component of the Coriolis acceleration), the governing equations are

$$\partial_t^2\nabla^2\psi + N^2\partial_x^2\psi + f^2\partial_z^2\psi = -\partial_t J(\nabla^2\psi,\psi) - \frac{g}{\rho_0}\partial_x J(\rho,\psi) - f\partial_z J(v,\psi), \tag{1}$$

$$\partial_t\rho + J(\rho,\psi) + \frac{\rho}{g}N^2\partial_x\psi = 0, \tag{2}$$

$$\partial_t v + J(v,\psi) + f\partial_z\psi = 0, \tag{3}$$

where $\nabla^2 \equiv \partial_x^2 + \partial_z^2$ and the Jacobian is $J(a,b) \equiv (\partial_x a)(\partial_z b) - (\partial_x b)(\partial_z a)$, as given by [29,31]. The mean fluid density is ρ_0, and ρ is the density change due to the velocity field. Gravity is aligned with the vertical (z) axis. Viscosity and diffusion are neglected. If the Jacobian terms are neglected, these equations reduce to the standard linear equations solved for a density staircase by [18].

Following the approach of [30], weakly nonlinear theory is used to calculated the perturbation to a single plane internal wave due to the variations in buoyancy frequency. The solution is decomposed into a linear solution ψ_0, with frequency ω and horizontal wave number k, and a (smaller amplitude) perturbation $\delta\psi$, as

$$\psi(x,z,t) = [\psi_0(z)e^{i(kx-\omega t)} + \text{c.c.}] + \delta\psi(x,z,t), \tag{4}$$

where ψ and $\delta\psi$ are real, ψ_0 is complex, and c.c. denotes complex conjugate. The density ρ and velocity component v are similarly decomposed. Inserting Eq. (4) into Eq. (1), the primary solution obeys the standard linear equation

$$\partial_z^2\psi_0 + k^2\frac{N^2-\omega^2}{\omega^2-f^2}\psi_0 = 0. \tag{5}$$

As shown in [30], the perturbation $\delta\psi$ obeys

$$\partial_t^2\nabla^2\delta\psi + N^2\partial_x^2\delta\psi + f^2\partial_z^2\delta\psi = -\frac{k^3}{\omega}\frac{4\omega^2-f^2}{\omega^2-f^2}(\partial_z N^2)\left[\psi_0^2 e^{2i(kx-\omega t)} + \text{c.c.}\right] + \frac{2f^2k^3}{\omega(\omega^2-f^2)}[2(N^2-\omega^2)\partial_z|\psi_0|^2 - (\partial_z N^2)|\psi_0|^2] \tag{6}$$

to lowest order in ψ_0. In uniform stratification ($\partial_z N^2 = 0$), there is no forcing for $\delta\psi$ (note that $\partial_z|\psi_0| = 0$ for a plane wave in this case) and the primary wave is an exact solution [32].

Equation (6) shows that any internal wave refracting in vertically varying stratification (nonzero $\partial_z N^2$), such as a density staircase, generates harmonics. These may be bound harmonics of the incident wave or freely propagating waves. Mathematically, Eq. (6) is analogous to a system of forced simple harmonic oscillators with forcing frequency 2ω and wave number $2k$.

The focus here will be on the steady-state forced (or bound) harmonic solution of Eq. (6). The steady-state bound harmonic solution is found by substituting $\delta\psi = \delta\psi_s(z)\exp[2i(kx - \omega t)] + \text{c.c.}$ into Eq. (6):

$$\partial_z^2 \delta\psi_s + (2k)^2 \frac{N^2 - (2\omega)^2}{(2\omega)^2 - f^2}\delta\psi_s = \frac{k^3}{\omega}\frac{\partial_z N^2}{(\omega^2 - f^2)}\psi_0^2. \tag{7}$$

Solutions to Eqs. (5) and (7) will be calculated for a density staircase in Sec. III. Such solutions could be realized if a distant source generates the linear solution ψ_0 for a long period of time, allowing the steady-state harmonic solution within the staircase to emerge from any initial transients. It is also assumed that the linear solution amplitude is small enough that higher-order nonlinear effects can be neglected. The amplitude of the steady-state harmonic depends on the proximity of the forcing frequency and wave number (double the incident wave values) to the freely propagating internal wave solutions of the staircase. Incident waves whose harmonic forcing is sufficiently close to a freely propagating wave will elicit a significant harmonic response (analogous to a forced oscillator), while nonlinear effects will be negligible for those which are not. Such near-resonant conditions are a special case of triadic resonances in nonuniform stratifications [29], with the linear wave comprising two components of the triad and the harmonic response being the third. This possibility of nonlinear dynamics within the staircase will, in some cases, complicate the linear picture of wave reflection and transmission found in [18].

III. STAIRCASE SOLUTION

The oceanic thermohaline staircase is represented here with an idealized stratification profile. Outside the density staircase, the buoyancy frequency is N_0. The step spacing is L and each step consists of a mixed layer ($N = 0$) with thickness $L - \delta$ and a thin layer boundary with thickness δ and buoyancy frequency N_p. The top and bottom boundary layers have thickness $\frac{1}{2}\delta$, so the mean buoyancy frequency across the staircase is N_0, as in [18]. The top of the staircase is arbitrarily defined as $z = 0$ and the full profile for a staircase with J mixed layers is given by

$$N(z) = \begin{cases} N_0, & z > 0 \\ N_p, & -\frac{1}{2}\delta < z < 0 \\ 0, & -jL + \frac{1}{2}\delta < z < -(j-1)L - \frac{1}{2}\delta, \quad j = 1, \ldots, J \\ N_p, & -jL - \frac{1}{2}\delta < z < -jL + \frac{1}{2}\delta, \quad j = 1, \ldots, J-1 \\ N_p, & -JL < z < -JL + \frac{1}{2}\delta \\ N_0, & z < -JL. \end{cases} \tag{8}$$

The mean density gradient across the staircase corresponds to the undisturbed stratification N_0, which yields the constraint $N_p^2\delta = N_0^2 L$. Figure 1 illustrates this profile for a staircase with $J = 3$ mixed layers. In the limit $\delta \to 0$ with $N_p^2\delta$ finite, the staircase profile reduces to that of [18]. Here the finite-thickness layer boundaries are used to accurately calculate the harmonic perturbation, but the limit $\delta \to 0$ will ultimately be taken.

A. Linear solution

The solution of Eq. (5) for a linear plane wave incident from above was previously found in [18] for the density staircase of Eq. (8) with $\delta \to 0$. Here the equivalent solution for finite δ is obtained

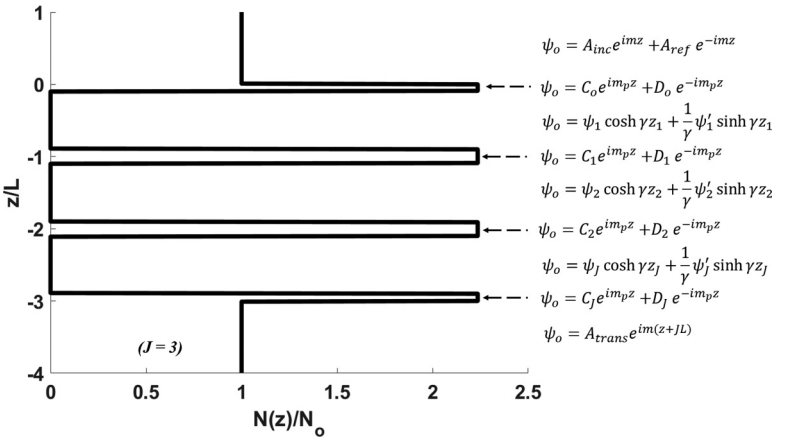

FIG. 1. Example stratification profile (8) and linear solution (10) for $J = 3$.

using the same matching conditions at the layer boundaries

$$\Delta[\psi_0] = \Delta[\partial_z \psi_0] = 0, \tag{9}$$

where $\Delta[\cdots]$ denotes the change in the bracketed quantity across the layer boundary. These correspond to the requirements that pressure and vertical velocity be continuous [18]. Because finite-thickness layer boundaries are used, these matching conditions do not involve density changes across the boundaries (unlike [18]).

For $f < \omega < N_0$, the plane-wave solution takes the form

$$\psi_0(z) = \begin{cases} A_{\text{inc}} \exp(imz) + A_{\text{ref}} \exp(-imz), & z > 0 \\ C_0 \exp(im_p z) + D_0 \exp(-im_p z), & -\frac{1}{2}\delta < z < 0 \\ \psi_j \cosh \gamma z_j + \gamma^{-1} \psi'_j \sinh \gamma z_j, & 0 < z_j < L - \delta, \quad j = 1, \ldots, J \\ C_j \exp(im_p z_j) + D_j \exp(-im_p z_j), & -\delta < z_j < 0, \quad j = 1, \ldots, J-1 \\ C_J \exp[im_p(z + JL)] + D_J \exp[-im_p(z + JL)], & -JL < z < -JL + \frac{1}{2}\delta \\ A_{\text{trans}} \exp[im(z + JL)], & z < -JL, \end{cases} \tag{10}$$

where the vertical coordinate within each layer is defined as

$$z_j \equiv z + jL - \tfrac{1}{2}\delta. \tag{11}$$

Here A_{inc} gives the complex amplitude of the incident plane wave (assumed without loss of generality to be incident from above), A_{ref} the reflected wave, and A_{trans} the transmitted wave. The structure of the solution segments is illustrated along with the stratification profile in Fig. 1 for $J = 3$. The vertical wave numbers m and m_p and the evanescent decay scale γ are given by

$$\gamma^2 \equiv k^2 \frac{\omega^2}{\omega^2 - f^2}, \tag{12}$$

$$m^2 \equiv k^2 \frac{N_0^2 - \omega^2}{\omega^2 - f^2}, \tag{13}$$

$$m_p^2 \equiv k^2 \frac{N_p^2 - \omega^2}{\omega^2 - f^2}. \tag{14}$$

The remaining (complex) coefficients in Eq. (10) are determined by the matching conditions (9). At boundaries between layers within the staircase ($j \neq 0$ or J), these conditions at $z = -jL + \frac{1}{2}\delta$ (or $z_j = 0$) yield

$$\psi_j = C_j + D_j, \tag{15}$$

$$\psi_j' = im_p(C_j - D_j), \tag{16}$$

while $z = -jL - \frac{1}{2}\delta$ (or $z_j = -\delta$ and $z_{j+1} = L - \delta$) gives

$$c\psi_{j+1} + s\gamma^{-1}\psi_{j+1}' = C_j \exp(-im_p\delta) + D_j \exp(im_p\delta), \tag{17}$$

$$s\gamma\psi_{j+1}' + c\psi_{j+1}' = im_p[C_j \exp(-im_p\delta) - D_j \exp(im_p\delta)], \tag{18}$$

$$c \equiv \cosh\gamma(L - \delta), \tag{19}$$

$$s \equiv \sinh\gamma(L - \delta). \tag{20}$$

These equations can be combined to eliminate the coefficients C_j and D_j, yielding the relationship between the stream function coefficients ψ_j and ψ_j' within each layer:

$$\begin{pmatrix} \psi_j \\ \frac{1}{\gamma}\psi_j' \end{pmatrix} = \mathbf{M}\begin{pmatrix} \psi_{j+1} \\ \frac{1}{\gamma}\psi_{j+1}' \end{pmatrix},$$

$$\mathbf{M} \equiv \begin{pmatrix} c\cos(m_p\delta) + s\frac{\gamma}{m_p}\sin(m_p\delta) & s\cos(m_p\delta) + c\frac{\gamma}{m_p}\sin(m_p\delta) \\ s\cos(m_p\delta) - c\frac{m_p}{\gamma}\sin(m_p\delta) & c\cos(m_p\delta) - s\frac{m_p}{\gamma}\sin(m_p\delta) \end{pmatrix}. \tag{21}$$

Similar conditions are obtained from the matching conditions for the layers at the top ($j = 0$) and bottom ($j = J$) of the staircase. Solving these for $j = 0$ yields

$$A_{\text{inc}} = \mathbf{V}_{\text{inc}}\begin{pmatrix} \psi_1 \\ \frac{1}{\gamma}\psi_1' \end{pmatrix}, \tag{22}$$

$$\mathbf{V}_{\text{inc}} \equiv \frac{1}{2}\begin{pmatrix} \left(c - i\frac{s\gamma}{m}\right)\cos\frac{1}{2}m_p\delta + \left(s\frac{\gamma}{m_p} + ic\frac{m_p}{m}\right)\sin\frac{1}{2}m_p\delta \\ \left(s - i\frac{c\gamma}{m}\right)\cos\frac{1}{2}m_p\delta + \left(c\frac{\gamma}{m_p} + is\frac{m_p}{m}\right)\sin\frac{1}{2}m_p\delta \end{pmatrix}, \tag{23}$$

$$A_{\text{ref}} = \mathbf{V}_{\text{ref}}\begin{pmatrix} \psi_1 \\ \frac{1}{\gamma}\psi_1' \end{pmatrix}, \tag{24}$$

$$\mathbf{V}_{\text{ref}} \equiv \frac{1}{2}\begin{pmatrix} \left(c + i\frac{s\gamma}{m}\right)\cos\frac{1}{2}m_p\delta + \left(s\frac{\gamma}{m_p} - ic\frac{m_p}{m}\right)\sin\frac{1}{2}m_p\delta \\ \left(s + i\frac{c\gamma}{m}\right)\cos\frac{1}{2}m_p\delta + \left(c\frac{\gamma}{m_p} - is\frac{m_p}{m}\right)\sin\frac{1}{2}m_p\delta \end{pmatrix}. \tag{25}$$

Likewise, the matching conditions at $z = -JL$ give

$$\begin{pmatrix} \psi_J \\ \frac{1}{\gamma}\psi_J' \end{pmatrix} = \mathbf{V}_{\text{trans}}A_{\text{trans}}, \tag{26}$$

$$\mathbf{V}_{\text{trans}} \equiv \begin{pmatrix} \cos\left(\frac{1}{2}m_p\delta\right) + i\frac{m}{m_p}\sin\left(\frac{1}{2}m_p\delta\right) \\ -\frac{m_p}{\gamma}\sin\left(\frac{1}{2}m_p\delta\right) + i\frac{m}{\gamma}\cos\left(\frac{1}{2}m_p\delta\right) \end{pmatrix}. \tag{27}$$

Combining these results relates the incident and transmitted wave amplitudes

$$A_{\text{inc}} = \mathbf{V}_{\text{inc}}^{\mathbf{T}}\mathbf{M}^{J-1}\mathbf{V}_{\text{trans}}A_{\text{trans}}. \tag{28}$$

This is equivalent to the plane-wave solution of [18], except that the matrices have been generalized for finite layer boundary thicknesses δ. As in [18], the relationship between the (known) incident wave amplitude A_{inc} and the transmitted wave A_{trans} can be found from the eigenvalues of the matrix $\mathbf{M}$.

B. Harmonic perturbation

Assuming $N_0 < 2\omega < N_p$, the steady-state harmonic perturbation takes the form

$$\delta\psi_s(z) = \begin{cases} \delta A_0 \exp(-m_H z), & z > 0 \\ \delta C_0 \exp(i m_{pH} z) + \delta D_0 \exp(-i m_{pH} z), & -\frac{1}{2}\delta < z < 0 \\ \delta\psi_j \cosh\gamma_H z_j + \gamma_H^{-1}\delta\psi_j' \sinh\gamma_H z_j, & 0 < z_j < L-\delta, \quad j = 1,\ldots,J \\ \delta C_j \exp(i m_{pH} z_j) + \delta D_j \exp(-i m_{pH} z_j), & -\delta < z_j < 0, \quad j = 1,\ldots,J-1 \\ \delta C_J \exp[i m_{pH}(z+JL)] + \delta D_J \exp[-i m_{pH}(z+JL)], & -JL < z < -JL + \frac{1}{2}\delta \\ \delta A_{J+1} \exp[m_H(z+JL)], & z < -JL. \end{cases} \tag{29}$$

Here δA_0 and δA_{J+1} are the amplitudes of the evanescent waves (for $2\omega > N_0$) above and below the staircase, respectively. The vertical wave numbers and evanescent decay scale are given by

$$\gamma_H^2 \equiv (2k)^2 \frac{(2\omega)^2}{(2\omega)^2 - f^2}, \tag{30}$$

$$m_H^2 \equiv (2k)^2 \frac{(2\omega)^2 - N_0^2}{(2\omega)^2 - f^2}, \tag{31}$$

$$m_{pH}^2 \equiv (2k)^2 \frac{N_p^2 - (2\omega)^2}{(2\omega)^2 - f^2}. \tag{32}$$

Although written for $2\omega > N_0$, it is straightforward to generalize to $2\omega < N_0$ by allowing m_H to be complex. In this case, δA_0 and δA_{J+1} represent the amplitudes of harmonic waves radiating away from the staircase.

The matching conditions for the harmonic solution at the layer boundaries ($z = -jL$) are given by [30]

$$\Delta[\delta\psi_s] = 0, \tag{33}$$

$$\Delta[\partial_z \delta\psi_s] = \frac{k^3}{\omega(\omega^2 - f^2)} \Delta[N^2]\psi_0^2. \tag{34}$$

The second requirement is obtained by integrating Eq. (7) across the layer boundary. The forcing of the harmonic by the primary wave occurs on the layer boundaries, where N^2 changes. The amplitude of the forcing is determined by the value of ψ_0^2 on each boundary within the staircase.

As in the linear solution, the matching conditions (33) and (34) at layer boundaries within the staircase ($j \neq 0$ or J) yield relations between the harmonic amplitudes ($\delta\psi_j$ and $\delta\psi_j'$) of

neighboring layers

$$\begin{pmatrix} \delta\psi_j \\ \frac{1}{\gamma_H}\delta\psi'_j \end{pmatrix} = \mathbf{M_H}\begin{pmatrix} \delta\psi_{j+1} \\ \frac{1}{\gamma_H}\delta\psi'_{j+1} \end{pmatrix} + \mathbf{F}_j,$$

$$\mathbf{M_H} \equiv \begin{pmatrix} c_H\cos(m_{pH}\delta) + s_H\frac{\gamma_H}{m_{pH}}\sin(m_{pH}\delta) & s_H\cos(m_{pH}\delta) + c_H\frac{\gamma_H}{m_{pH}}\sin(m_{pH}\delta) \\ s_H\cos(m_{pH}\delta) - c_H\frac{m_{pH}}{\gamma_H}\sin(m_{pH}\delta) & c_H\cos(m_{pH}\delta) - s_H\frac{m_{pH}}{\gamma_H}\sin(m_{pH}\delta) \end{pmatrix},$$

$$\mathbf{F}_j \equiv \frac{k^3N_p^2}{\omega(\omega^2-f^2)}\begin{pmatrix} \frac{\sin(m_{pH}\delta)}{m_{pH}}\big(\cos(m_p\delta)\psi_j - \frac{\sin(m_p\delta)}{m_p}\psi'_j\big)^2 \\ \gamma_H^{-1}\cos(m_{pH}\delta)\big(\cos(m_p\delta)\psi_j - \frac{\sin(m_p\delta)}{m_p}\psi'_j\big)^2 - \gamma_H^{-1}\psi_j^2 \end{pmatrix},$$

$$c_H \equiv \cosh\gamma_H(L-\delta),$$

$$s_H \equiv \sinh\gamma_H(L-\delta). \tag{35}$$

This result is analogous to Eq. (22) for the linear solution, except for the nonzero forcing term. For $\mathbf{F} = 0$, this reduces to Eq. (22) but the wave number and frequency are $2k$ and 2ω. Solutions for the harmonic will therefore be resonant if $(2k, 2\omega)$ is a freely propagating mode of the system (i.e., it lies on the linear wave dispersion curve). The harmonic forcing depends on the change in buoyancy frequency at the layer boundaries and the value of the primary wave stream function ψ_j and ψ'_j on the layer boundaries. Equation (35) gives a total of $2J-2$ constraints for the $2J$ unknowns: $\delta\psi_j$ and $\delta\psi'_j$ $(1 \leqslant j \leqslant J)$.

The two remaining constraints needed to determine the harmonic solution are found by considering the matching conditions at $j = 0$ and $j = J$, which also determine the evanescent wave amplitudes δA_0 and δA_{J+1}. These constraints are

$$\begin{pmatrix} \big(c_H + s_H\frac{\gamma_H}{m_H}\big)\cos\frac{1}{2}m_{pH}\delta + \big(s_H\frac{\gamma_H}{m_{pH}} - c_H\frac{m_{pH}}{m_H}\big)\sin\frac{1}{2}m_{pH}\delta \\ \big(s_H + c_H\frac{\gamma_H}{m_H}\big)\cos\frac{1}{2}m_{pH}\delta + \big(c_H\frac{\gamma_H}{m_{pH}} - s_H\frac{m_{pH}}{m_H}\big)\sin\frac{1}{2}m_{pH}\delta \end{pmatrix}\begin{pmatrix} \delta\psi_1 \\ \frac{1}{\gamma_H}\delta\psi'_1 \end{pmatrix}$$

$$= \frac{k^3N_p^2}{\omega(\omega^2-f^2)m_H}\left[(A_{\rm inc}+A_{\rm ref})^2 - (c\psi_1 + s\gamma^{-1}\psi'_1)^2\left(\cos\frac{1}{2}m_{pH}\delta + \frac{m_H}{m_{pH}}\sin\frac{1}{2}m_{pH}\delta\right)\right]$$

$$- \frac{k^3N_0^2}{\omega(\omega^2-f^2)m_H}(A_{\rm inc}+A_{\rm ref})^2 \tag{36}$$

and

$$\begin{pmatrix} \cos\frac{1}{2}m_{pH}\delta - \frac{m_{pH}}{m_H}\sin\frac{1}{2}m_H\delta \\ -\frac{\gamma_H}{m_H}\cos\frac{1}{2}m_{pH}\delta - \frac{\gamma_H}{m_{pH}}\sin\frac{1}{2}m_{pH}\delta \end{pmatrix}\begin{pmatrix} \delta\psi_J \\ \frac{1}{\gamma_H}\delta\psi'_J \end{pmatrix}$$

$$= \frac{k^3N_0^2}{\omega(\omega^2-f^2)m_H}A_{\rm trans}^2 + \frac{k^3N_p^2}{\omega(\omega^2-f^2)m_H}$$

$$\times\left[\psi_J^2\left(\cos\frac{1}{2}m_{pH}\delta + \frac{m_H}{m_{pH}}\sin\frac{1}{2}m_{pH}\delta\right) - A_{\rm trans}^2\right]. \tag{37}$$

The evanescent wave amplitudes (radiated for $2\omega < N_0$) outside the staircase are

$$\delta A_0 = \left(c_H\cos\frac{1}{2}m_{pH}\delta + s_H\frac{\gamma_H}{m_{pH}}\sin\frac{1}{2}m_{pH}\delta\right)\delta\psi_1$$

$$+ \left(s_H\cos\frac{1}{2}m_{pH}\delta + c_H\frac{\gamma_H}{m_{pH}}\sin\frac{1}{2}m_{pH}\delta\right)\gamma_H^{-1}\delta\psi'_1$$

$$+\frac{1}{m_{pH}}\sin\left(\frac{1}{2}m_{pH}\delta\right)\frac{k^3N_p^2}{\omega(\omega^2-f^2)}(c\psi_1+s\gamma^{-1}\psi_1')^2, \tag{38}$$

$$\delta A_{J+1}=\cos\left(\frac{1}{2}m_p\delta\right)\delta\psi_J-\frac{1}{m_{pH}}\sin\left(\frac{1}{2}m_{pH}\delta\right)\left(\frac{1}{\gamma_H}\delta\psi_J'+\frac{k^3N_p^2}{\omega(\omega^2-f^2)}\psi_J^2\right). \tag{39}$$

Given the primary wave solution (ψ_j,ψ_j'), the linear set of algebraic equations (35)–(37) can be inverted to yield the harmonic solution $(\delta\psi_j,\delta\psi_j')$. The harmonic amplitudes on the staircase boundaries are then given by the auxiliary conditions of Eqs. (38) and (39).

C. Thin interface ($\delta\to 0$) limit

The general solutions for finite-thickness layer boundaries given in the preceding section simplify greatly in the limit $\delta\to 0$. This reduces the parameter space to be explored and is relevant to oceanic staircases because double-diffusive convection tends to maintain thin boundaries. However, it typically will not apply to laboratory experiments such as [17] for which the layer boundaries are not thin compared to L. For $\delta\to 0$, with the constraint $N_p^2\delta=N_0^2L$, the following limits apply:

$$\begin{aligned}\cos m_p\delta &\to 1,\\ \frac{1}{m_p}\sin m_p\delta &\to \delta\to 0,\\ m_p\sin m_p\delta &\to m_p^2\delta\to\frac{N_0^2Lk^2}{\omega^2-f^2}.\end{aligned} \tag{40}$$

Using these in the primary wave solution, the matrix $\mathbf{M}$ in Eq. (22) reduces to

$$\begin{aligned}\mathbf{M}&\to\begin{pmatrix}c & s\\ s-2c\Gamma & c-2s\Gamma\end{pmatrix},\\ \Gamma&\equiv\frac{N_0^2L}{2\gamma}\frac{k^2}{\omega^2-f^2},\end{aligned} \tag{41}$$

while the vectors for computing the incident, reflected, and transmitted wave amplitudes are given by

$$\begin{aligned}\mathbf{V}_{\text{inc}}&\to\frac{1}{2}\begin{pmatrix}c-i\frac{\gamma}{m}(s-c\Gamma)\\ s-i\frac{\gamma}{m}(c-s\Gamma)\end{pmatrix},\\ \mathbf{V}_{\text{ref}}&\to\frac{1}{2}\begin{pmatrix}c+i\frac{\gamma}{m}(s-c\Gamma)\\ s+i\frac{\gamma}{m}(c-s\Gamma)\end{pmatrix},\\ \mathbf{V}_{\text{trans}}&\to\begin{pmatrix}1\\ -\Gamma+i\frac{m}{\gamma}\end{pmatrix}.\end{aligned} \tag{42}$$

Inserting these in Eq. (28) yields the primary wave solution in the limit $\delta\to 0$. The solution is equivalent to that found by [18], as shown in the Appendix.

The harmonic solution uses limits analogous to Eq. (40), but with m_{pH} replacing m_p. Using these limits, the constraints within the staircase are given by Eq. (35), with the matrix $\mathbf{M_H}$ and forcing $\mathbf{F}_j$

given by

$$\mathbf{M_H} \to \begin{pmatrix} c_H & s_H \\ s_H - 2c_H\Gamma_H & c_H - 2s_H\Gamma_H \end{pmatrix},$$
$$\mathbf{F}_j \to \frac{2k\gamma\Gamma}{\omega}\psi_j \begin{pmatrix} \psi_j \\ -\frac{2}{\gamma_H}\psi_j' \end{pmatrix}, \tag{43}$$
$$\Gamma_H \equiv \frac{N_0^2 L}{2\gamma_H}\frac{4k^2}{4\omega^2 - f^2}.$$

The harmonic solution is analogous to the linear solution, except for the forcing terms given by the values of the linear solution on the interfaces (ψ_j, ψ_j'). Likewise, the constraints at the top (36) and bottom (37) reduce to

$$\left[c_H\left(\frac{m_H}{\gamma_H} - \Gamma_H\right) + s_H\right]\delta\psi_1 + \left[s_H\left(\frac{m_H}{\gamma_H} - \Gamma_H\right) + c_H\right]\frac{1}{\gamma_H}\delta\psi_1'$$
$$= -\frac{2k\gamma\Gamma}{\omega\gamma_H L}(c\psi_1 + s\gamma^{-1}\psi_1')\left\{\left[c\left(1 + \frac{1}{2}m_H L\right) - s\gamma L\right]\psi_1 + \left[s\left(1 + \frac{1}{2}m_H L\right) - c\gamma L\right]\gamma^{-1}\psi_1'\right\}, \tag{44}$$

$$\left(\frac{m_H}{\gamma_H} - \Gamma_H\right)\delta\psi_J - \frac{1}{\gamma_H}\delta\psi_J' = \frac{k\gamma\Gamma}{\omega\gamma_H L}(2 + m_H L + 2imL)\psi_J^2. \tag{45}$$

The harmonic solution in the limit $\delta \to 0$ is obtained by inverting the linear algebraic set of equations (43)–(45). Once this solution has been found, the harmonic wave amplitudes outside the density staircase are given by

$$\delta A_0 = c_H\delta\psi_1 + s_H\gamma_H^{-1}\delta\psi_1' + \frac{k\Gamma\gamma}{\omega}(c\psi_1 + s\gamma^{-1}\psi_1')^2, \tag{46}$$
$$\delta A_{J+1} = \delta\psi_J - \frac{k\Gamma\gamma}{\omega}\psi_J^2. \tag{47}$$

For $2\omega > N_0$ these waves outside the density staircase are evanescent; otherwise they are radiating waves with double the incident wave frequency and wave number.

IV. RESULTS

The weakly nonlinear harmonic generated by an incident plane wave depends on the frequency and wave number of the incident wave. These quantities are expressed here in dimensionless terms as kL and ω/N_0, respectively. In addition, the number of steps J in the staircase and the rotation frequency f/N_0 are also factors in the dynamics. The amplitude of the harmonic response is proportional to the amplitude squared $|A_{\text{inc}}|^2$ of the incident wave, as is typical for weakly nonlinear effects. Here, all results presented are for the $\delta \to 0$ solution found in the preceding section; finite δ is not considered.

Harmonic solutions differ qualitatively depending on whether the incident wave energy is mostly transmitted through the density staircase, or mostly reflected. The linear solution of [18] yields an approximate threshold wave number kL for transmission, which depends on ω/N_0. Smaller wave numbers (larger wavelengths) generally have linear transmission coefficients T which approach one, while larger wave numbers are mostly reflected ($T \to 0$). There are exceptions due to constructive and destructive interference within the staircase, as described in [18]. Details of the vertical structure of the harmonic solution, as well as its amplitude, are explored below as a function of the characteristics of the incident wave and the density staircase.

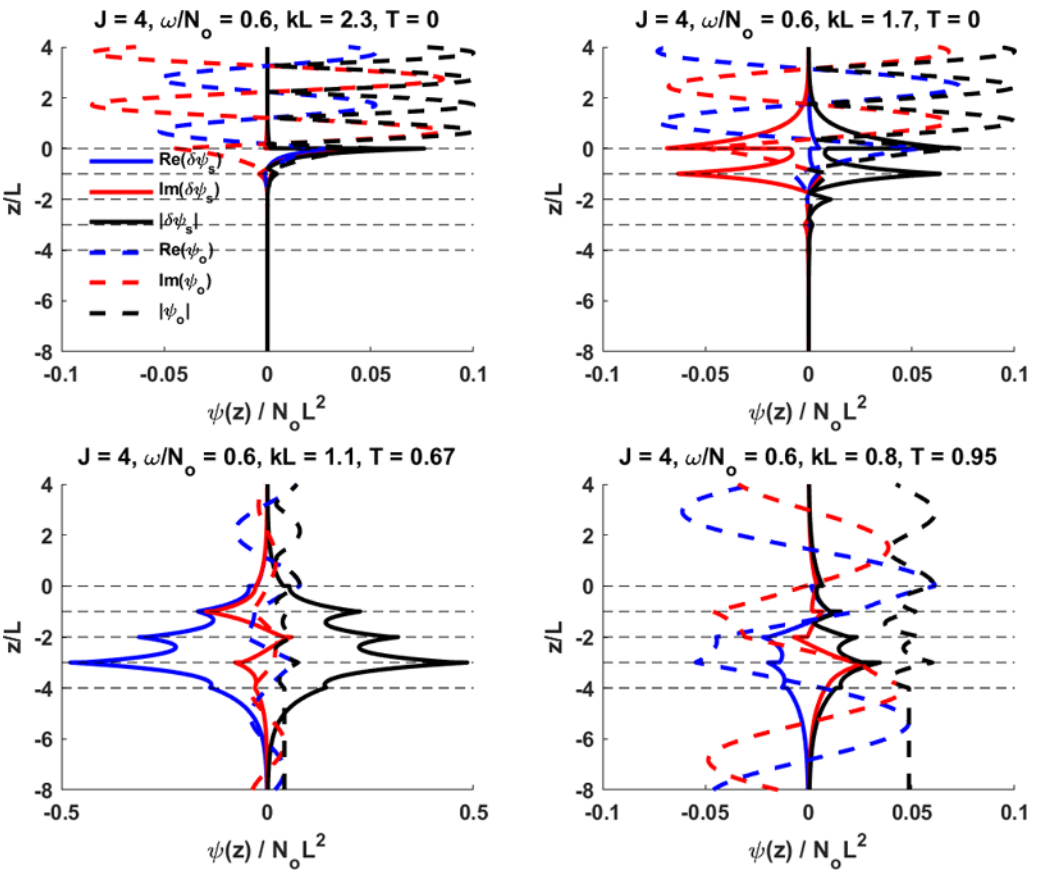

FIG. 2. Stream function profiles for the steady-state harmonic perturbation $\delta\psi_s(z)$ (solid lines) and primary (linear) wave $\psi_0(z)$ (dotted lines) in a staircase with $J = 4$ and incident wave amplitude $|A_{\text{inc}}| = 0.05N_0L^2$. The harmonic perturbation is trapped in the staircase for this incident frequency ($\omega = 0.6N_0$). There is no rotation ($f = 0$).

A. Example profiles for $2\omega > N_0$

Figure 2 presents example stream function profiles for a staircase with $J = 4$ layers. (This value of J was selected as it is large enough to yield examples representative of staircases with many steps, but small enough for concise graphical representation.) In all cases the incident frequency is $\omega = 0.6N_0$, so the harmonic mode is evanescent outside the staircase. There is no rotation ($f = 0$). Dashed lines denote the primary wave solution, while solid lines indicate the harmonic perturbation. Black curves show the absolute value of the stream function, while blue and red show the real and imaginary parts, respectively. In all cases the incident wave amplitude $|A_{\text{inc}}|$ is $0.05N_0L^2$, a value selected to be representative of small-scale oceanic internal waves. Oceanic stratifications are typically on the order of 0.002 rad/s (one to three cycles per hour, in standard oceanographic units) and typical staircase layer sizes are a few meters [1–3]. The value of A_{inc} used in Fig. 2 ($0.05N_0L^2$) corresponds to an oceanic wave with a stream function amplitude of $\sim 5 \times 10^{-4}$ m^2/s. The corresponding vertical velocities (kA_{inc}) are on the order of 1 mm/s and vertical displacements (kA_{inc}/ω) are on the order of 10 cm (much less than the layer size L). The harmonic amplitude is proportional to the square of the incident amplitude, so the relative amplitudes of the primary and harmonic waves depend on the value of A_{inc}.

Profiles for four incident wave numbers kL are shown. The title of each panel indicates the value of kL and the linear transmission coefficient T for that case. (Complete reflection has $T = 0$, while complete transmission has $T = 1$, neglecting nonlinear effects.) The top row shows two examples of incident wavelengths which are $\simeq$3 times the mixed-layer thickness ($kL \simeq 2$) and the incident wave is completely reflected ($|\psi_0| \simeq 0$ for $z < -JL$). In the top left panel, the harmonic perturbation consists of an interfacial wave confined to the upper boundary of the staircase ($z = 0$). In this case, the dynamics are approximately equivalent to the pycnocline harmonics previously investigated in the laboratory experiments of [22–24] and the numerical simulations of [25–27]. The lower steps of the staircase have no significant effect on the harmonic. In the top right panel, the incident wave (dashed lines) partially penetrates into the staircase, although it does not completely tunnel through it. This excites a second interfacial wave propagating along the next layer boundary ($z = -L$), along with the wave on the top of the staircase ($z = 0$). This illustrates the qualitatively different nonlinear feature of the density staircase, compared to a single interface: the richer structure of harmonic modes allowed by the primary wave interacting with the many layers of the staircase. It is also worth noting that the phase of the harmonic mode (indicated by the relative values of the real and imaginary parts) differs between the two cases shown in the top row by nearly 180° (solid red and blue lines).

The bottom row of Fig. 2 presents example profiles for cases in which the incident wave is mostly transmitted through the staircase ($T \to 1$). In the bottom left panel, the harmonic amplitude within the density staircase consists of several interfacial waves, the strongest of which is found on the $z = -3L$ interface. The harmonic stream function (solid lines) is an order of magnitude larger than the primary wave (dashed lines) for the chosen incident wave amplitude. This occurs because the harmonic forcing frequency and wave number lie in close proximity to a freely propagating mode of the density staircase. Although the weakly nonlinear assumption fails for this particular incident wave amplitude, the solution profile shown could be realized for a weaker incident wave. The bottom right panel shows a case with nearly complete transmission. The harmonic profile shape is similar to that of the bottom left panel, but the amplitude is reduced by more than an order of magnitude. This amplitude reduction occurs because the forcing wave number has moved away from the freely propagating staircase mode.

B. Example profiles for $2\omega < N_0$

Figure 3 presents example profiles for incident waves with a frequency $\omega = 0.3N_0$. Since $2\omega \leqslant N_0$ in this case, the harmonic perturbation is not confined to the staircase, but can radiate away in either direction. As in Fig. 2, the incident wave amplitude is $|A_{\text{inc}}| = 0.05N_0L^2$ and there is no rotation ($f = 0$). The line types are the same as in Fig. 2 and the incident horizontal wave number kL and corresponding transmission coefficient T are indicated at the top of each panel. The top row presents two cases in which the incident wave is completely reflected ($T \simeq 0$). In the top left panel, a harmonic wave radiates above the staircase, along with the reflected primary wave. For this incident wave amplitude, the two waves are comparable in amplitude. In the top right panel, the incident wavelength is longer and it partially penetrates into the staircase (but is not transmitted). The radiated harmonic is much weaker than in the top left panel, but the harmonic is stronger within the staircase (at $z \simeq -J$) because of the deeper incident wave penetration.

The bottom row of Fig. 3 presents two examples in which most of the incident wave energy is linearly transmitted through the staircase ($T \simeq 1$). In both cases, the harmonic amplitude is largest within the staircase, but radiated harmonics are also present both above and below the staircase. In the bottom left panel, the radiated harmonic above the staircase has an amplitude about triple that of the radiated harmonic below the staircase. In the bottom right panel, the two radiated harmonics have nearly identical amplitudes.

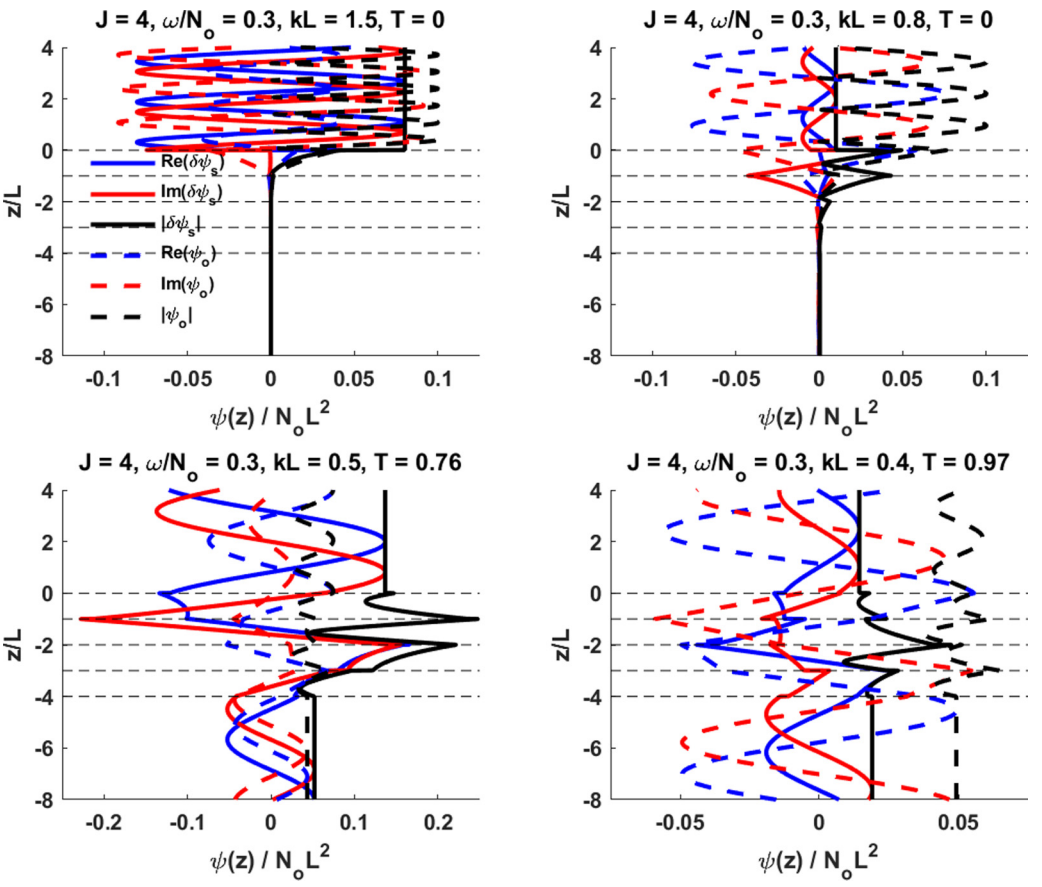

FIG. 3. Stream function profiles for the steady-state harmonic perturbation $\delta\psi_s(z)$ (solid lines) and linear solution $\psi_0(z)$ (dotted lines) in a staircase with $J = 4$ and incident wave amplitude $|A_{\text{inc}}| = 0.05N_0L^2$. The harmonic perturbation radiates away from the staircase for this incident frequency ($\omega = 0.3N_0$). There is no rotation ($f = 0$).

C. Parameter dependence of the harmonic solution

Figures 2 and 3 illustrate the richness and complexity of the harmonics than may be generated by internal waves incident on a density staircase. However, they do not provide a systematic understanding of the complete parameter space of possible nonlinear harmonic excitations. Figure 4 presents one measure of the harmonic amplitude as a function of incident wave number kL and frequency ω/N_0 for four different staircase sizes ($J = 1$, 2, 4, and 10) without rotation. The color scale shows the logarithm (base 10) of the dimensionless harmonic amplitude at the top of the staircase, $\log_{10}(\frac{\omega|\delta A_0|}{|kA_{\text{inc}}|^2})$. This quantity gives the ratio of the harmonic stream function amplitude to the square of the incident wave stream function amplitude. For this weakly nonlinear process, this ratio is independent of $|A_{\text{inc}}|$. Also shown in Fig. 4 are two curves. The dashed black line cutting diagonally across each panel indicates the approximate boundary between linear reflection and transmission found in [18],

$$\left(\frac{\omega}{N_0}\right)^2 = \frac{1}{2}kL\tanh\frac{1}{2}kL. \tag{48}$$

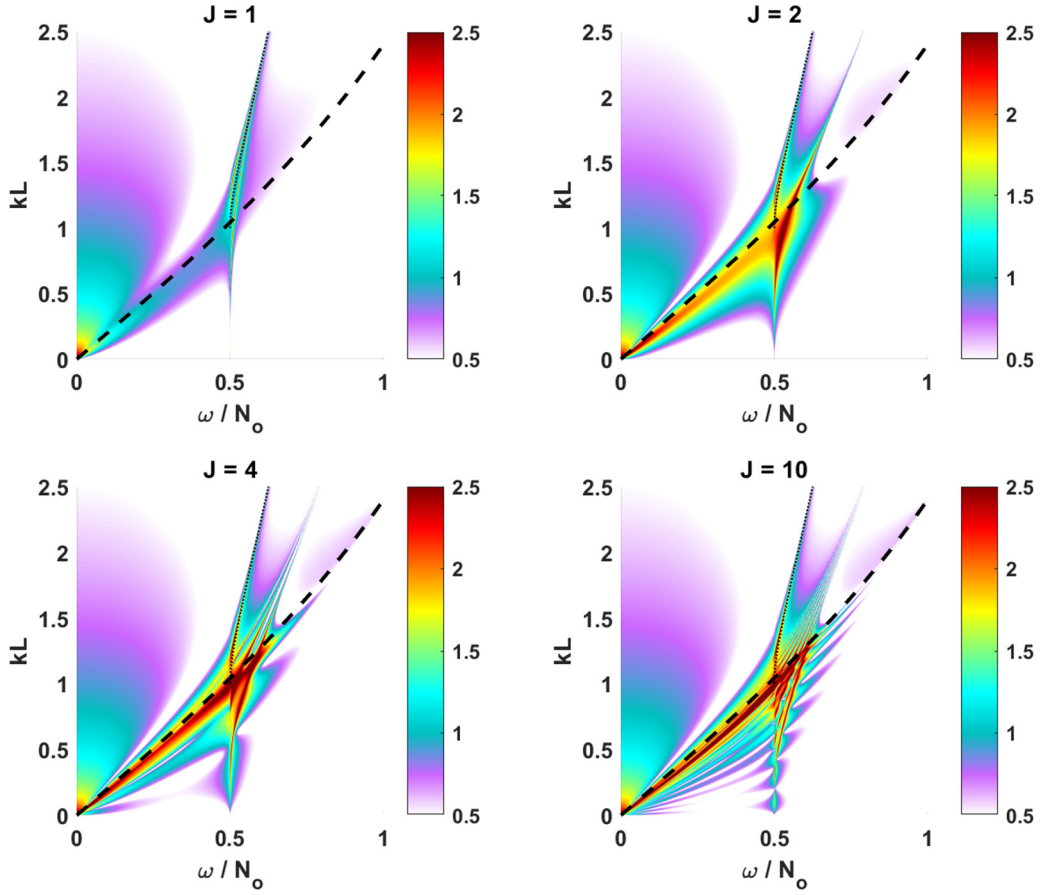

FIG. 4. Dimensionless steady-state harmonic amplitude at the staircase top ($\omega|\delta A_0|/|kA_{\rm inc}|^2$) on a logarithmic (base 10) scale as a function of incident wave frequency ω/N_0 and wave number kL for staircases with one, two, four, and ten steps. The dashed black line shoes the approximate linear wave transmission boundary (reflection above, transmission below), while the dotted black line shows the pycnocline interfacial harmonic resonance criteria from [27].

Incident waves with kL above this line are predominantly reflected in linear theory, while those with longer wavelengths (below the dashed black line) are predominantly transmitted. The other curve is the nonlinear harmonic interfacial wave resonance curve derived in [27] for a plane wave incident on a pycnocline above an infinite-thickness mixed layer:

$$kL = \frac{4\omega}{N_0}\left(\frac{\omega}{N_0} + \sqrt{\frac{\omega^2}{N_0^2} - \frac{1}{4}}\right). \tag{49}$$

This curve is indicated by a dotted black line, which originates at the linear reflection-transmission boundary for $\omega = 0.5N_0$ and extends upward. The interfacial wave does not exist for $\omega < 0.5N_0$. In the limit $kL \to \infty$, the staircase dynamics studied here reduces to the infinite-mixed-layer case investigated in [27].

The case of a single layer ($J = 1$) is presented in the top left panel. In this case, the harmonic response is largest for three distinct regions. One can be found along along the linear reflection-transmission boundary (indicated by the dashed black line) for $\omega < 0.5N_0$. For these solutions, the harmonic is a radiated wave. Another is found along the interfacial harmonic resonance curve

of [27]. Here the harmonic is an interfacial wave propagating along the upper boundary of the staircase and the dynamics are essentially identical to the previously studied case of harmonic generation on an isolated pycnocline. The third region of harmonic activity is found at very small ω/N_0 for wavelengths longer than the step size ($kL < \sim 2$) and also consists of radiated waves.

The harmonic modal structure increases in complexity as more layers are added to the staircase, as illustrated in the other panels of Fig. 4. Adding additional layers increases the amplitude of the radiated harmonic generated by waves near the linear reflection-transmission boundary (dashed black line). The single interfacial harmonic mode corresponding to the solution of [27] (dotted black line) is not altered significantly by additional layers, because the incident wave does not penetrate deeply into the staircase, nor are the radiated harmonics for very small ω/N_0 altered. Adding layers to the staircase allows new harmonic modes to occur in the transmission region near $\omega \simeq 0.5N_0$. These correspond to collective excitations of interfacial waves on multiple layers of the staircase, as illustrated in Fig. 2. These modes occur only for incident waves which penetrate the staircase (necessary to generate waves on interior interfaces) and only for trapped wave frequencies. The complexity of this modal structure increases as layers are added. Above the linear transmission boundary, there is a second region of harmonic activity which lies to the right of the single interfacial wave curve (dotted black line). These modes correspond to an interfacial wave on the upper boundary (as in [27]) but with a dispersion relation that is altered by interaction with weaker waves traveling along interior interfaces. An example stream function profile for these modes is shown in the top right panel of Fig. 2. The number of allowed modes in this regime increases as layers are added to the staircase, but they are closely packed in kL-ω/N_0 space.

To put the color scale used in Fig. 4 in an oceanic context, note that the harmonic amplitude can be expressed in terms of the plotted ratio as

$$\frac{|\delta A_0|}{|A_{\text{inc}}|} = \frac{(kL)^2}{\omega/N_0}\frac{|A_{\text{inc}}|}{N_0L^2}\left(\frac{\omega|\delta A_0|}{|kA_{\text{inc}}|^2}\right). \tag{50}$$

For oceanic internal waves, $\frac{|A_{\text{inc}}|}{N_0L^2}$ is typically of order 0.01 to 0.1, as stated above. Since kL and ω/N_0 are both of order unity over most of Fig. 4, this implies that the yellow and red regions (ratios greater than $\simeq$30) would have $|\delta A_0| \sim |A_{\text{inc}}|$ for typical internal waves incident on an oceanic density staircase. For these parameter values, weakly nonlinear theory indicates that harmonic generation will have a significant impact on steady-state wave dynamics in a density staircase.

The amplitude ratio presented in Fig. 4 is only one measure of the harmonic response to a plane wave incident on a density staircase. For $\omega < 0.5N_0$, it gives the amplitude of the harmonic wave radiated upward, while for larger ω it gives the amplitude of the interfacial wave on the upper boundary. However, in either case it provides no information on the dynamics in the interior of the density staircase. This is especially important if the harmonic solution is confined to the staircase ($\omega > 0.5N_0$). To better explore the harmonic response across the full staircase, consider the mean kinetic energy density of the harmonic solution within the density staircase. This is given by

$$\langle \delta K \rangle \equiv \frac{1}{2JL}\int_{-JL}^{0}(|k\delta\psi_s|^2 + |\partial_z\delta\psi_s|^2)dz. \tag{51}$$

This is evaluated using Eq. (29) for $\delta \to 0$, yielding

$$\langle \delta K \rangle = k^2\frac{8\omega^2 - f^2}{4\omega^2 - f^2}\frac{\sinh 2\gamma_H L}{\gamma_H L}\frac{1}{J}\sum_j\left(|\delta\psi_j| + \left|\gamma_H^{-1}\delta\psi_j'\right|\right)^2$$
$$- \frac{2k^2f^2}{4\omega^2 - f^2}\frac{1}{J}\sum_j\left(|\delta\psi_j|^1 + \left|\gamma_H^{-1}\delta\psi_j'\right|^1\right). \tag{52}$$

The harmonic kinetic energy density is compared to that of the incident wave

$$\langle K_{\text{inc}} \rangle \equiv (k^2 + m^2)|A_{\text{inc}}|^2 \tag{53}$$

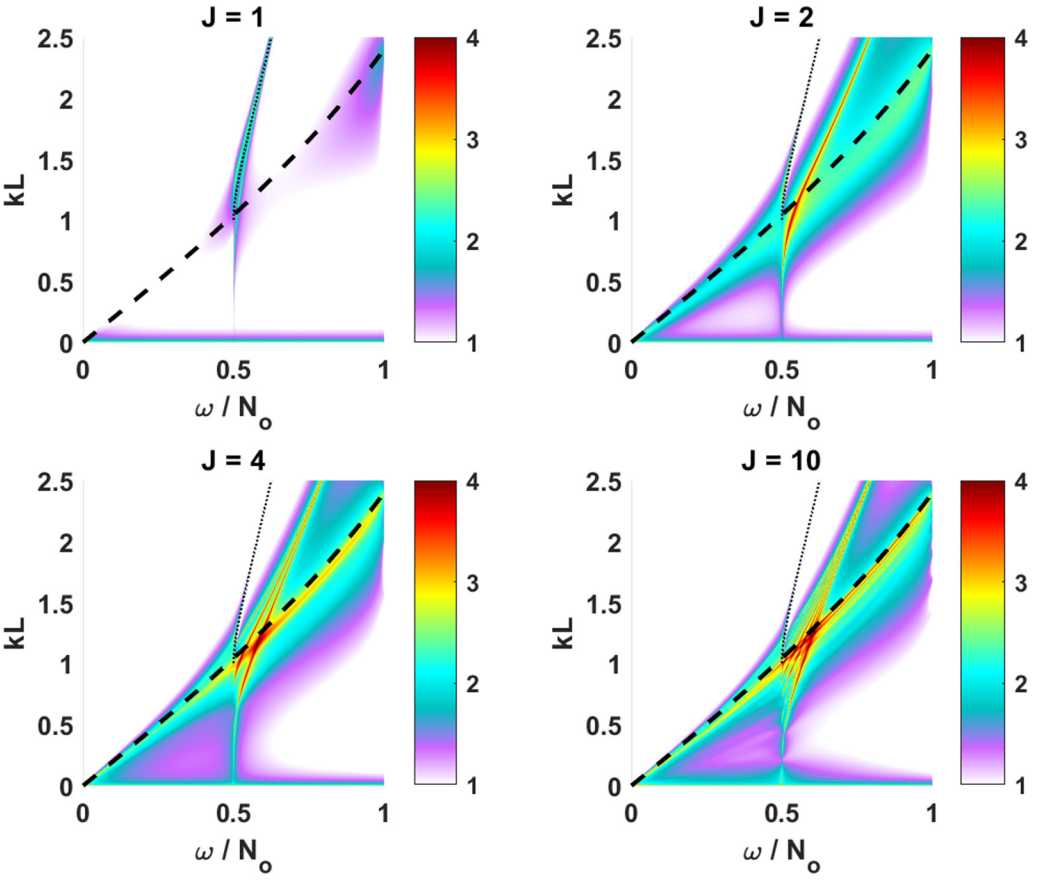

FIG. 5. Dimensionless steady-state staircase kinetic energy ratio R_K as a function of incident wave frequency ω/N_0 and wave number kL for staircases with one, two, four, and ten steps. The dashed black line shoes the approximate linear wave transmission boundary (reflection above, transmission below), while the dotted black line shows the pycnocline interfacial harmonic resonance criteria from [27].

by defining the ratio

$$R_K \equiv \frac{\omega\sqrt{\langle \delta K \rangle}}{k^2 \langle K_{\text{inc}} \rangle}. \tag{54}$$

Like the amplitude ratio at the top of the staircase presented in Fig. 4, this ratio is independent of the incident wave amplitude A_{inc}.

Figure 5 presents the mean kinetic energy density ratio R_K on a logarithmic scale, over the same parameter space as in Fig. 4. Comparing the two figures, there is a striking difference at low ω. Although there can be a significant harmonic radiated from the upper boundary, Fig. 5 shows that there is very little harmonic energy within the density staircase. This is because the incident wave does not penetrate into the staircase. The trapped interfacial harmonic mode on the upper staircase boundary (found along the dotted black line) also becomes less prominent as the number of steps increases, compared to Fig. 4. Again, this is because the primary wave does not penetrate into the staircase, so harmonic energy is confined to the uppermost interface, which represents a decreasing fraction of the total staircase as the number of steps increases. On the other hand, the area along and below the transmission boundary (dashed black line) for $\omega > 0.5N_0$ has significant kinetic energy in the harmonic mode, exceeding what was indicated in Fig. 4. In this case, much of the harmonic energy is found in the interior of the density staircase.

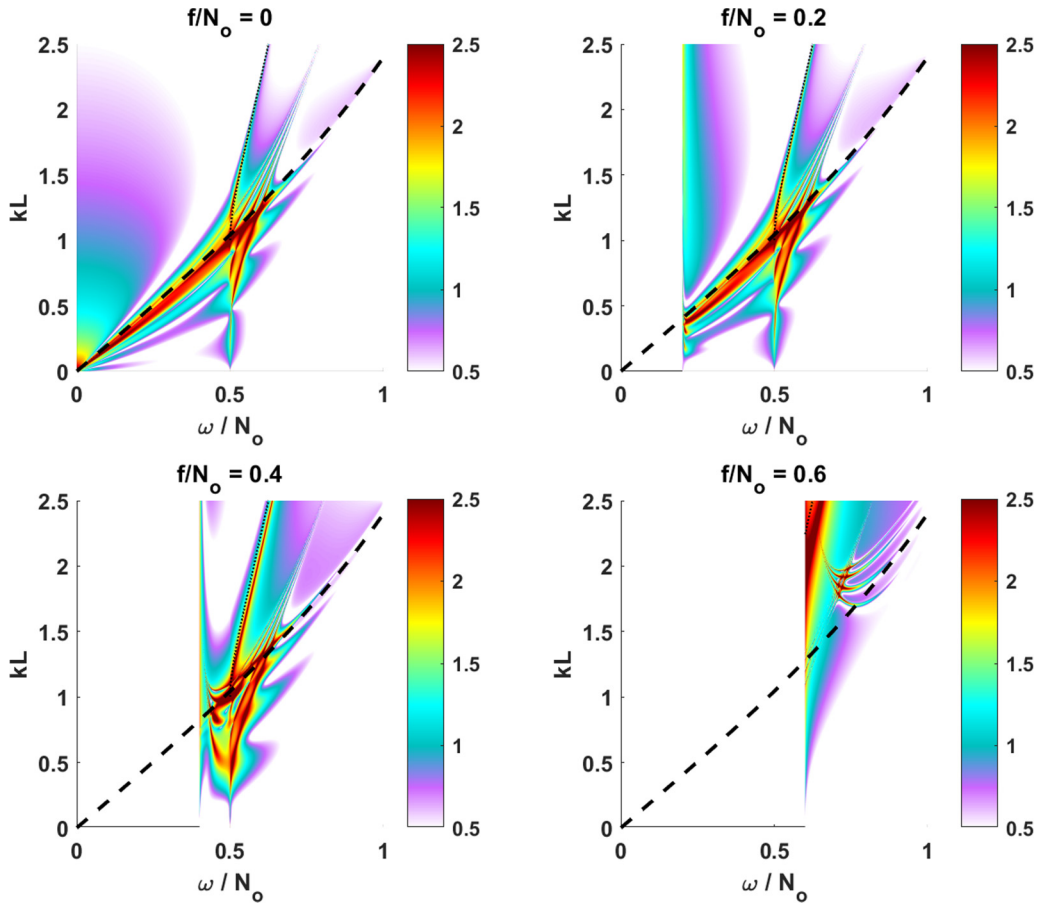

FIG. 6. Dimensionless steady-state harmonic amplitude at the staircase top ($\omega|\delta A_0|/|kA_{\rm inc}|^2$) on a logarithmic (base 10) scale as a function of incident wave frequency ω/N_0 and wave number kL for four different rotation frequencies f/N_0 in a staircase with $J = 5$ steps.

The effect of rotation on the harmonic solution, which may be important for Arctic density staircases, is presented in Fig. 6 for a staircase with $J = 5$ steps. Incident waves only exist for $\omega > f$. For small values of f/N_0, rotation has little effect for values of ω which are more than about $0.1N_0$ larger than f. Rotation does alter the low-ω radiated harmonic, enhancing it for near-inertial waves ($\omega \simeq f$). As the rotation frequency f approaches $0.5N_0$, the structure of the trapped harmonic modes is noticeably altered by the rotation. For $f > 0.5N_0$, the effect of rotation on the trapped harmonic modes is significant.

V. DISCUSSION

The linear solution of [18] for plane internal waves incident on a density staircase has been extended into the weakly nonlinear regime. The resulting steady-state perturbation to the linear solution consists of a forced harmonic with double the incident wave frequency and wave number. Forcing occurs on the interfaces separating mixed layers within the staircase, due to the gradients in buoyancy frequency found there. Two qualitatively distinct types of harmonic responses were found. For incident wave frequencies $\omega < 0.5N_0$, harmonic plane waves radiate away from the density staircase. In cases where the linear solution is completely reflected, the harmonic wave radiates in the same direction, since forcing is limited to one side of the staircase. If the incident

wave is transmitted through the staircase, forcing occurs on both the upper and lower staircase boundaries, resulting in radiated harmonic waves in both directions. For $\omega > 0.5N_0$, the harmonic solution is confined to the density staircase and consists of one or more interfacial waves traveling along the boundaries between staircase mixed layers. As the number of steps within the staircase increases, the number and complexity of these coupled harmonic interfacial wave modes increase. This is especially true when the incident wave is transmitted through the staircase so that forcing occurs on all interfaces.

In all cases, the magnitude of the harmonic response to an incident plane wave depends strongly on the proximity of the forcing frequency and wave number to the freely propagating modes of the system. Incident waves which are nearly resonant with a freely propagating wave can generate a harmonic with significant amplitude. In some cases, the steady-state solution derived here may fail because the harmonic amplitude is too large for the weakly nonlinear approximation to be valid. Incident waves with a forcing frequency and wave number which do not fall in the vicinity of a freely propagating wave generally do not generate harmonics of any consequence, and in those cases the linear steady-state solution of [18] is not altered by nonlinear effects.

For oceanic internal waves, the results presented indicate that a significant harmonic response could plausibly occur for some incident wave numbers and frequencies. Interfacial wave harmonics with steady-state amplitudes that are a significant fraction of the incident wave amplitude are found along multiple bands, primarily with incident wave numbers in the range $\sim 0.5 < kL < \sim 1$ and frequencies in the range $0.5 < \omega/N_0 < \sim 0.7$. These ranges correspond to horizontal wavelengths of tens of meters and wave periods on the order of an hour. The strongest radiated harmonics ($\omega < 0.5N_0$) are found along the linear wave transmission boundary calculated in [18], given by Eq. (48). However, for horizontal wavelengths longer than $\sim$100 m ($kL < \sim 0.1$), the ocean surface would alter both the linear and weakly nonlinear solutions for real oceanic thermohaline staircases, which are typically found at depths of a few hundred meters or less.

Thermohaline staircases in the ocean might provide a mechanism for converting some internal wave energy to higher frequencies and wave numbers, through radiated harmonic waves. Some internal wave energy could also be trapped within the staircase in the form of interfacial waves. An internal wave which in linear theory would be transmitted through the staircase without loss might instead lose some energy to its harmonic. Increased internal wave energy incident on Arctic staircases, as has been suggested due to decreasing sea ice cover [17], could alter the dynamics of the staircase. It is perhaps conceivable that trapped interfacial wave modes could achieve sufficiently large vertical displacements to impact the stability of Arctic thermohaline staircases.

The present results are limited to single plane waves in steady state (i.e., continuously forced). The transient development of the forced harmonic modes requires either an extension of the present approach, analogous to that of [30], or fully nonlinear numerical simulations, analogous to those of [33]. For near-resonant forcing, rapid growth of the harmonic is plausible, based on similar weakly nonlinear results for low-mode internal tides with a single interface [30], although a full analysis is needed to determine this.

The present results also apply only to a single plane wave and neglect nonlinear wave-wave interactions which would occur when a spectrum of internal waves is incident upon a staircase. Previous studies of an internal wave beam incident on a single thin interface have suggested that wave-wave interactions may be more important than the harmonic forcing mechanism considered here for radiated harmonics ($\omega < 0.5N_0$), but that the harmonic forcing mechanism is dominant for interfacial wave generation ($\omega > 0.5N_0$) [24,26,27]. In those studies, for $\omega > 0.5N_0$ the incident beam excited only the harmonic wave number which was resonant with an interfacial wave. By analogy, one might expect a spectrum of internal waves incident on an ocean staircase to excite the freely propagating modes found by the present analysis for $\omega > 0.5N_0$, with the steady-state amplitude of each harmonic determined by the amplitude of the incident forcing wave number and frequency.

ACKNOWLEDGMENT

Helpful discussions with Professor Bruce Sutherland are gratefully acknowledged.

APPENDIX: LINEAR SOLUTION

The linear solution presented here differs in form from that of [18]. This was done to conveniently express the harmonic forcing in terms of the values of the primary (linear) solution on the interfaces, ψ_j and ψ'_j. Here it is shown that the present solution is equivalent to that of [18] for $\delta \to 0$. The linear solution in the interior of the staircase is expressed here as

$$\begin{pmatrix} \psi_j \\ \frac{1}{\gamma}\psi'_j \end{pmatrix} = \mathbf{M}\begin{pmatrix} \psi_{j+1} \\ \frac{1}{\gamma}\psi'_{j+1} \end{pmatrix}, \tag{A1}$$

$$\mathbf{M} = \begin{pmatrix} c & s \\ s - 2c\Gamma & c - 2s\Gamma \end{pmatrix}, \tag{A2}$$

where $c \equiv \cosh \gamma L$ and $s \equiv \sinh \gamma L$.

In [18], the solution is written as

$$\begin{pmatrix} A_j \\ B_j \end{pmatrix} = \mathbf{C}\begin{pmatrix} A_{j+1} \\ B_{j+1} \end{pmatrix}, \tag{A3}$$

$$\mathbf{C} = \begin{pmatrix} e^{\gamma L}(1-\Gamma) & -\Gamma \\ \Gamma & e^{-\gamma L}(1+\Gamma) \end{pmatrix}. \tag{A4}$$

The solution ψ_0 within each layer is written as

$$\psi_0(z_j) = \psi_j \cosh \gamma z_j + \gamma^{-1}\psi'_j \sinh \gamma z_j = A_j \exp\left[\gamma\left(z_j - \tfrac{1}{2}L\right)\right] + B_j \exp\left[-\gamma\left(z_j - \tfrac{1}{2}L\right)\right], \tag{A5}$$

where the first expression (in terms of ψ_j and ψ'_j) is used in the present paper, while the second expression (in terms of A_j and B_j) is used in [18]. The two sets of parameters are related by

$$\begin{pmatrix} A_j \\ B_j \end{pmatrix} = \mathbf{T}\begin{pmatrix} \psi_{j+1} \\ \frac{1}{\gamma}\psi'_{j+1} \end{pmatrix}, \tag{A6}$$

$$\mathbf{T} = \frac{1}{2}\begin{pmatrix} \exp\left(\frac{1}{2}\gamma L\right) & \exp\left(\frac{1}{2}\gamma L\right) \\ \exp\left(-\frac{1}{2}\gamma L\right) & -\exp\left(-\frac{1}{2}\gamma L\right) \end{pmatrix}. \tag{A7}$$

By substitution, the solution of [18] can be written in terms of the present variables as

$$\begin{pmatrix} \psi_j \\ \frac{1}{\gamma}\psi'_j \end{pmatrix} = \mathbf{T}^{-1}\mathbf{C}\mathbf{T}\begin{pmatrix} \psi_{j+1} \\ \frac{1}{\gamma}\psi'_{j+1} \end{pmatrix}, \tag{A8}$$

where the inverse of $\mathbf{T}$ is

$$\mathbf{T}^{-1} = \begin{pmatrix} \exp\left(-\frac{1}{2}\gamma L\right) & \exp\left(\frac{1}{2}\gamma L\right) \\ \exp\left(-\frac{1}{2}\gamma L\right) & -\exp\left(\frac{1}{2}\gamma L\right) \end{pmatrix}. \tag{A9}$$

After some straightforward but tedious algebra, the matrix multiplication yields

$$\mathbf{T}^{-1}\mathbf{C}\mathbf{T} = \mathbf{M}, \tag{A10}$$

demonstrating that the two solutions are equivalent. The same can be shown for the conditions on the top ($j = 0$) and bottom ($j = J$) of the staircase.

[1] R. W. Schmitt, Double diffusion in oceanography, Annu. Rev. Fluid Mech. **26**, 255 (1994).
[2] D. E. Kelly, H. J. S. Fernando, A. E. Gargett, J. Tanny, and E. Ozsoy, The diffusive regime of double-diffusive convection, Prog. Oceanogr. **56**, 461 (2003).
[3] J. Carpenter and M.-L. Timmermans, Temperature steps in salty seas, Phys. Today **65**(3), 66 (2012).
[4] R. A. Woodgate, K. Aagaard, J. H. Swift, W. M. Smethie, and K. K. Falkner, Atlantic water circulation over the Mendeleev Ridge and Chukchi Borderland from thermohaline intrusions and water mass properties, J. Geophys. Res. **112**, C02005 (2007).
[5] L. Rainville and P. Winsor, Mixing across the Arctic Ocean: Microstructure observations during the Beringia 2005 Expedition, Geophys. Res. Lett. **35**, L08606 (2008).
[6] M.-L. Timmermans, J. Toole, R. Krishfield, and P. Winsor, Ice-tethered profiler observations of the double-diffusive staircase in the Canada Basin thermocline, J. Geophys. Res. **113**, C00A02 (2008).
[7] M.-L. Timmermans, S. Cole, and J. Toole, Horizontal density structure and restratification of the Arctic Ocean surface layer, J. Phys. Oceanogr. **42**, 659 (2012).
[8] T. D. Foster and E. C. Carmack, Temperature and salinity structure in the Wedell Sea, J. Phys. Oceanogr. **6**, 36 (1976).
[9] R. D. Muench, H. J. S. Fernando, and G. R. Stegen, Temperature and salinity staircases in the Northwesten Wedell Sea, J. Phys. Oceanogr. **20**, 295 (1990).
[10] E. Ozsoy, U. Unluata, and Z. Top, The Mediterranean water evolution, material transport by double diffusive intrusions, and interior mixing in the Black Sea, Prog. Oceanogr. **31**, 275 (1993).
[11] O. M. Johannessen and O. S. Lee, A deep stepped thermo-haline structure in the Mediterranean, Deep-Sea Res. **21**, 629 (1974).
[12] P. A. Mazeika, Subsurface mixed layers in the northwest tropical Atlantic, J. Phys. Oceanogr. **4**, 446 (1974).
[13] R. B. Lambert and W. Sturges, A thermohaline staircase and vertical mixing in the thermocline, Deep-Sea Res. **24**, 211 (1977).
[14] R. W. Schmitt, H. Perkins, J. D. Boyd, and M. C. Stalcup, C-SALT: An investigation of the thermohaline staircase in the western tropical North Atlantic, Deep-Sea Res. **34**, 1655 (1987).
[15] J. C. Swallow and J. Crease, Hot salty water at the bottom of the Red Sea, Nature (London) **205**, 165 (1965).
[16] L. Rainville, C. M. Lee, and R. A. Woodgate, Impact of wind-driven mixing in the Arctic Ocean, Oceanography **24**, 136 (2011).
[17] S. J. Ghaemsaidi, H. V. Dosser, L. Rainville, and T. Peacock, The impact of multiple layering on internal wave transmission, J. Fluid Mech. **789**, 617 (2016).
[18] B. R. Sutherland, Internal wave transmission through a thermohaline staircase, Phys. Rev. Fluids **1**, 013701 (2016).
[19] W. J. Merryfield, Hydrodynamics of semiconvection, Astrophys. J. **444**, 318 (1995).
[20] M. A. Balyaev, E. Quataert, and J. Fuller, The properties of g-modes in layered semiconvection, Mon. Not. R. Astron. Soc. **452**, 2700 (2015).
[21] Q. André, A. J. Barker, and S. Mathis, Layered semiconvection and tides in giant planet interiors. I. Propagation of internal waves, Astron. Astrophys. **605**, A117 (2017).
[22] M. J. Mercier, M. Mathur, L. Gostiaux, T. Gerkema, J. M. Magalhaes, J. C. B. da Silva, and T. Dauxois, Soliton generation by internal tidal beams impinging on a pycnocline: Laboratory experiments, J. Fluid Mech. **704**, 37 (2012).
[23] S. Wunsch and A. Brandt, Laboratory experiments on internal wave interactions with a pycnocline, Exp. Fluids **53**, 1663 (2012).
[24] S. Wunsch, I. Delwiche, G. Frederick, and A. Brandt, Experimental study of nonlinear harmonic generation by internal waves incident on a pycnocline, Exp. Fluids **56**, 87 (2015).
[25] N. Grisouard, C. Staquet, and T. Gerkema, Generation of internal solitary waves in a pycnocline by an internal wave beam: a numerical study, J. Fluid Mech. **676**, 491 (2011).
[26] S. Wunsch, H. Ku, I. Delwiche, and R. Awadallah, Simulations of nonlinear harmonic generation by an internal wave beam incident on a pycnocline, Nonlin. Process. Geophys. **21**, 855 (2014).

[27] P. J. Diamesses, S. Wunsch, I. Delwiche, and M. P. Richter, Nonlinear generation of harmonics through the interaction of an internal wave beam with a model oceanic pycnocline, Dyn. Atmos. Oceans **66**, 110 (2014).
[28] S. A. Thorpe, Nonlinear reflection of internal waves at a density discontinuity at the base of a mixed layer, J. Phys. Oceanog. **28**, 1853 (1998).
[29] D. Varma and M. Mathur, Internal wave resonant triads in finite-depth non-uniform stratifications, J. Fluid Mech. **824**, 286 (2017).
[30] S. Wunsch, Harmonic generation by nonlinear self-interaction of a single internal wave mode, J. Fluid Mech. **828**, 630 (2017).
[31] P. H. LeBlond and L. A. Mysak, *Waves in the Ocean* (Elsevier, Amsterdam, 1981).
[32] A. Tabaei, T. R. Akylas, and K. G. Lamb, Nonlinear effects in reflecting and colliding internal wave beams, J. Fluid Mech. **526**, 217 (2005).
[33] B. R. Sutherland, Excitation of superharmonics by internal modes in a non-uniformly stratified fluid, J. Fluid Mech. **793**, 335 (2016).